

IoT-Enabled Automatic Power Factor Controller using Arduino Uno and ESP32 with Zero-Crossing Detection and Real-Time Web Monitoring

Mr. Ramesh Papayya Mhanta¹, Mr. Vijay J. Patil²

M. Tech Student, Department of Electrical Engineering, Fabtech Technical Campus, College of Engineering and Research, Sangola, Dist. Solapur, Maharashtra, India¹

Assistant Professor, Department of Electrical Engineering, Fabtech Technical Campus, College of Engineering and Research, Sangola, Dist. Solapur, Maharashtra, India²

ABSTRACT: This paper presents the design, hardware implementation, and experimental validation of a low-cost Automatic Power Factor Controller (APFC) integrated with Internet of Things (IoT)-based real-time remote monitoring. The system employs zero-crossing detection (ZCD) circuits for both supply voltage and load current to compute the displacement power factor continuously on an Arduino Uno (ATmega328P) microcontroller. Based on the measured phase lag between voltage and current zero crossings, the controller automatically switches up to two relay-controlled capacitor banks to compensate reactive power and maintain power factor at or above 0.95 lagging. An ESP32 Wi-Fi module receives electrical parameter data from the Arduino over UART and serves a responsive HTML5 web dashboard accessible from any browser on the local network without internet dependency. The system also features a dual-mode operation — fully automatic capacitor switching and manual override via push buttons — with a 16×2 LCD for on-panel display. Experimental results confirm power factor improvement from 0.823 to 0.994 under mixed inductive-resistive loading at 230 V, 50 Hz, representing a 78.0% reduction in reactive power demand. The complete prototype cost is approximately INR 2,500, offering a practical and scalable solution for small industries and educational institutions.

KEYWORDS: Automatic power factor controller, zero-crossing detection, Arduino Uno, ESP32, IoT web server, capacitor bank switching, reactive power compensation, power quality, single-phase 230 V 50 Hz.

I. INTRODUCTION

Power factor (PF) is a fundamental index of efficiency in AC power systems, defined as the ratio of real power (W) to apparent power (VA). In industrial and commercial installations, a large proportion of loads are inductive — including motors, transformers, and fluorescent lamp ballasts — causing the load current to lag behind the supply voltage and driving PF well below unity [1]. Low PF imposes significant economic penalties: distribution companies in India levy surcharges on consumers whose average PF falls below 0.90, while consumers maintaining PF above 0.95 receive rebates [15]. Beyond economics, low PF increases feeder current, accelerates equipment wear, and reduces system capacity.

Conventional fixed-capacitor compensation fails to track dynamically varying reactive power demand, potentially causing over-compensation during light-load periods, which is equally harmful. Automatic Power Factor Controllers (APFCs) overcome this by continuously measuring PF and switching discrete capacitor stages in or out through relay or thyristor contactors [2, 3]. With the proliferation of the Internet of Things (IoT) and low-cost microcontroller platforms, there is growing interest in embedding remote monitoring directly into power correction equipment. Prior work has employed PIC microcontrollers [5], Arduino platforms [6], and ESP8266-based cloud loggers [9, 10]; however, these implementations are either limited to local display, dependent on external cloud platforms, or lack dual-mode operation. The proposed system bridges these gaps by integrating real-time ZCD-based PF measurement, intelligent two-stage capacitor switching, and an ESP32 Wi-Fi web server into a single cost-effective prototype.

The remainder of this paper is organized as follows. Section II reviews Literature Survey. Section III provides the theoretical basis. Section IV describes the hardware design. Section V covers the firmware and software. Section VI presents experimental results. Section VII concludes.

II. LITERATURE SURVEY

Early APFC implementations relied on dedicated analog phase-detection ICs coupled to thyristor contactors [1]. The shift to microcontroller-based designs enabled programmable switching logic, improved accuracy, and lower cost. Patil et al. [5] demonstrated a PIC16F877A-based APFC with four capacitor stages achieving PF correction from 0.72 to 0.97 on a single-phase test bench. Kumar and Singh [6] extended this approach to three-phase loads using Arduino Mega with eight relay-driven stages.

Shanmugam et al. [7] compared ZCD timing with ADC-sampling methods, establishing that ZCD outperforms ADC sampling for sinusoidal linear loads at 50 Hz. CT-116 and SCT-013 series current transformers have become the standard low-cost current sensing solution for such prototypes.

On the IoT front, Rajan et al. [9] deployed an ESP8266-Blynk energy monitor, while Sharma et al. [10] used ThingSpeak for cloud-based PF logging; both require continuous internet connectivity.

Pandey and Agarwal [11] used the ESP32 for a standalone local web server power quality analyzer, eliminating cloud dependency. The present work extends [11] by adding automatic capacitor switching, dual Auto/Manual mode, LCD local display, and a structured ZCD-based measurement pipeline — creating a fully integrated APFC+IoT system.

III. SYSTEM THEORY

A. Power Factor and Power Triangle

For a sinusoidal single-phase system, the displacement power factor is:

$$PF = \cos\phi = P / S = P / (V_{\text{rms}} \times I_{\text{rms}})$$

where P is real power (W), S is apparent power (VA), and ϕ is the phase angle between voltage and current phasors. The reactive power Q (VAR) is related by $S^2 = P^2 + Q^2$. The required capacitive reactive power to improve PF from PF_1 to PF_2 is:

$$Q^c = P \times (\tan\phi_1 - \tan\phi_2)$$

B. Zero-Crossing Detection Principle

For a 50 Hz supply (period $T = 20$ ms), the phase angle ϕ between voltage and current is directly proportional to the time lag t_{lag} between their positive zero crossings:

$$\phi = (t_{\text{lag}} / 20 \text{ ms}) \times 360^\circ \Rightarrow PF = \cos(t_{\text{lag}} \times 18^\circ/\text{ms})$$

A lag of 0–5 ms maps to lagging PF 1.0 to 0.0; a lag > 5 ms indicates leading (over-compensated) current. The Arduino firmware clamps t_{lag} to [0, 10] ms and computes $PF = \cos(\phi \text{ in radians})$ accordingly.

IV. SYSTEM DESIGN AND HARDWARE

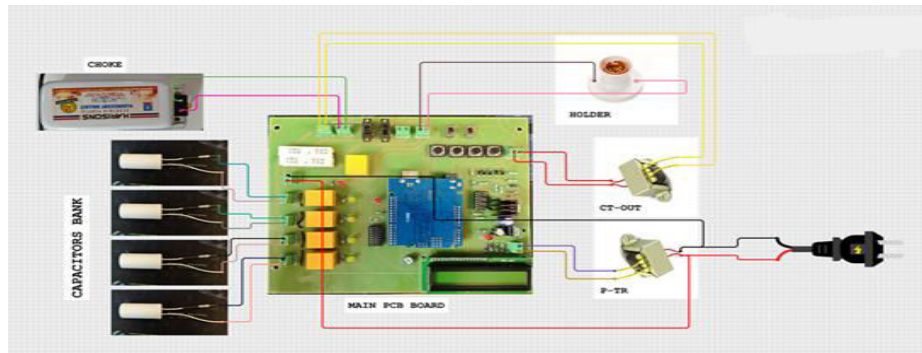


Fig. 1: APFC System Wiring Diagram - Complete Hardware Connection Overview

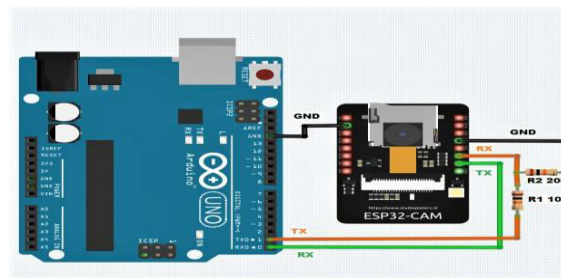


Fig. 2: Arduino Uno to ESP32-CAM UART Connection with R1/R2 Voltage Divider Level Shifter

A. System Architecture

The proposed APFC system consists of five functional subsystems working in an integrated manner:

1. Sensing Subsystem: Voltage ZCD circuit (P-TR: potential transformer + comparator) and Current ZCD circuit (CT-116 current transformer) detect zero crossings of supply voltage and load current respectively. The CT secondary also provides an analog voltage for ADC-based RMS current measurement.
2. Processing Subsystem: Arduino Uno microcontroller (ATmega328P, 16 MHz) measures the time difference between zero crossings, calculates power factor, and determines the appropriate capacitor switching action.
3. Actuation Subsystem: Three electromagnetic relays (for CAP3, CAP4, and capacitive load) switch the correction capacitors and the inductive/capacitive test loads on and off.
4. Display Subsystem: A 16x2 LCD module (HD44780) connected to Arduino Uno in 4-bit mode displays real-time electrical parameters and system status on rotating screens.

IoT Monitoring Subsystem: Arduino Uno transmits electrical parameter data to an ESP32 module over UART at 9600 baud. The ESP32 serves a responsive HTML web dashboard accessible to any browser on the local Wi-Fi network

B. Hardware Components:- Table II lists the principal hardware components. The Arduino Uno interfaces with both the sensing and actuation subsystems through its 14 digital I/O pins and 6 analog inputs. The ESP32 uses its Hardware Serial 2 (GPIO16/17) for UART at 9600 baud from the Arduino, and its integrated 802.11 b/g/n radio for Wi-Fi. A resistive voltage divider (R1 = 10 kΩ, R2 = 20 kΩ) shifts the 5 V Arduino TX to approximately 3.33 V to protect the 3.3 V-tolerant ESP32 RX pin

C. ZCD Circuit Design :- The voltage ZCD uses the P-TR secondary (9 V RMS) fed through a bridge rectifier and LM393 comparator with a mid-rail reference, producing a 5 V TTL square wave phase-aligned to supply zero crossings, connected to Arduino D5.

The current ZCD uses the CT-116 secondary across a burden resistor network; the same LM393 comparator produces a TTL output on Arduino D6. The CT secondary is also rectified for ADC input on A5 for peak-detection RMS current measurement (9,000 samples per cycle).

D. Capacitor Bank Switching Logic :- Two polypropylene capacitor stages (CAP3 on relay D2, CAP4 on relay D3) provide three discrete compensation levels as per Table I. The 2.5 ms midpoint threshold divides the 0–5 ms lagging range into two equal correction zones, minimizing over- and under-compensation

TABLE I - Capacitor Switching Logic

Lag Time (ms)	CAP3	CAP4	Condition
0 or PF \geq 0.95	OFF	OFF	No correction needed
0 – 2.5	ON	OFF	Mild lag — partial comp.
\geq 2.5	ON	ON	Severe lag — full comp.

TABLE II Key Hardware Components and Specifications

S.No.	Component	Specification	Qty	Function
1	Arduino Uno R3	ATmega328P, 5V, 16MHz, 14 digital I/O, 6 analog	1	Main microcontroller
2	ESP32 Dev Module	Dual-core 240MHz, Wi-Fi 802.11 b/g/n, 3.3V I/O	1	IoT web server
3	CT-116 Current Transformer	1000:1 ratio, rated 5A primary, isolated output	1	Current sensing & ZCD
4	Step-Down Transformer (P-TR)	230V:9V, 500mA (Potential Transformer)	1	Voltage ZCD reference
5	Relay Module (CAP3)	5V coil, 10A/250VAC NO contact	1	Capacitor bank 3 switching
6	Relay Module (CAP4)	5V coil, 10A/250VAC NO contact	1	Capacitor bank 4 switching
7	Relay Module (CLRELAY)	5V coil, 10A/250VAC NO contact	1	Capacitive load switching
8	Capacitor Bank - CAP3	Polypropylene film, 230VAC rated	1	Reactive power stage 1
9	Capacitor Bank - CAP4	Polypropylene film, 230VAC rated	1	Reactive power stage 2
10	Inductive Load (Choke)	Harisons Fluorescent Ballast 40W, 50Hz	1	Inductive load simulation
11	Lamp Holder + Bulb	E27 holder, 60W incandescent lamp	1	Resistive load simulation
12	16x2 LCD Module	HD44780 compatible, 5V, 16-pin	1	Local parameter display
13	Push Buttons (BTN1, BTN2)	SPST momentary, active LOW	2	Manual cap switching

S.No.	Component	Specification	Qty	Function
14	Toggle Switches (AMSW, CLSW)	SPDT panel mount	2	Mode and load selection
15	Resistors R1=10k, R2=20k	0.25W resistors	1 set	5V to 3.3V level shifting for ESP32
16	Relay Driver (ULN2003)	Darlington array, 500mA per channel	1	Relay coil driving

V. SOFTWARE DESIGN

A. Arduino Firmware

The firmware is organized as a super-loop that alternates between Auto and Manual modes based on the mode switch state (PIN_AMSW). In Auto mode, `measurePhase()` polls D5 and D6 with 40 ms per-edge watchdog timeouts. The lag time between voltage and current positive zero crossings (timestamped via `micros()`) is converted to phase angle and PF. `measureCurrent()` performs 9,000 ADC samples on A5 to obtain peak ADC count, then derives $I_{\text{max}} = \text{adcPeak} / 512.9$, $S = 230 \times I_{\text{max}}$, $P = S \times \text{PF}$, and $Q = S \times \sin(\phi)$. `switchCaps(ilag)` actuates the relays per Table II. `sendToNodeMCU()` transmits "PF,IRMS,KVA,KW,KVAR,230.0 " over UART. In Manual mode, BTN1 and BTN2 control CAP3 and CAP4 directly.

The 40 ms timeout on each ZCD polling edge ensures safe behavior if sensor connections fail: PF defaults to 1.0, all relays remain de-energized, and the LCD displays "NO SIGNAL! Check ZCD wiring".

B. ESP32 Web Server

The ESP32 firmware (Arduino core) connects to a local Wi-Fi network in Station mode and runs a `WiFiServer` on port 80. On each incoming client connection, it assembles a complete HTTP/1.1 response containing an HTML5 page with embedded CSS. The Power Factor card applies conditional CSS classes (green: $\text{PF} \geq 0.95$; amber: $0.80-0.95$; red: < 0.80). A `<meta http-equiv="refresh" content="2">` tag causes the browser to reload every two seconds, providing near-real-time visibility without Websocket complexity or internet dependency.

The UART2 parser uses `String.indexOf()` and `String.substring()` to extract the six comma-separated float values (PF, I_{max} , S, P, Q, V) from each Arduino transmission. Both firmware modules were compiled in Arduino IDE 2.x with ESP32 Arduino Core v2.x.

VI. EXPERIMENTAL RESULTS AND DISCUSSION

A. Experimental Setup

The prototype was assembled on a custom single-sided PCB and powered from a standard 230 V, 50 Hz domestic supply. The inductive test load comprised a Harisons 40 W fluorescent lamp ballast (choke), presenting a highly inductive impedance at 50 Hz. A 60 W incandescent lamp was added as a resistive component to create a mixed load condition. The ESP32 was connected to a mobile Wi-Fi hotspot, and the dashboard was accessed from a laptop browser using the IP address printed on the Arduino serial monitor.

B. Power Factor Correction Results

Table III summarizes measured electrical parameters across all three switching states. Without correction, $\text{PF} = 0.823$ with 30.0 VAR reactive demand. Connecting CAP3 alone raised PF to 0.910; connecting both CAP3 and CAP4 achieved $\text{PF} = 0.994$ with only 6.6 VAR residual reactive power — a 78.0% reduction. Real power remained essentially constant, confirming purely reactive compensation with negligible active power disturbance.

TABLE III Measured Electrical Parameters — All Switching States

Parameter	No Caps	CAP3 Only	CAP3 CAP4 +
Power Factor	0.8235	0.9100	0.9940
Current I_{xmx} (A)	0.230	0.215	0.261
Apparent Power (VA)	52.9	49.5	60.1
Real Power (W)	43.6	45.0	59.7
Reactive Power (VAR)	30.0	21.5	6.6
Lag Time (ms)	~3.4	~2.1	~0.3
Phase Angle (°)	~61.2	~37.8	~5.4

C. Web Dashboard Output

The ESP32 web server successfully served the real-time monitoring dashboard on the local Wi-Fi network. The following screenshots capture the dashboard under two different operating conditions:

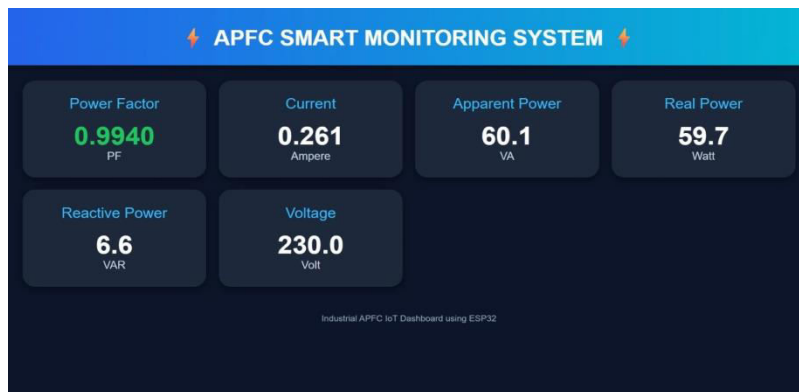


Fig. 3: ESP32 Web Dashboard showing PF = 0.9940 (Green indicator) - Both capacitor banks active, near-unity power factor achieved



Fig. 4: ESP32 Web Dashboard showing PF = 0.8235 (Amber indicator) - No capacitors connected, natural inductive load condition

The dashboard renders correctly on both desktop browsers and mobile devices due to the responsive CSS Grid layout with min-max column sizing. The color-coded Power Factor card provides immediate visual indication of power quality status: green (PF ≥ 0.95 - good), amber ($0.80 \leq \text{PF} < 0.95$ - needs attention), red (PF < 0.80 - poor, immediate correction needed). The 2-second auto-refresh provides near-real-time visibility without requiring any manual browser refresh action.

VII. CONCLUSION

This paper has presented and validated an IoT-enabled automatic power factor controller for single-phase 230 V, 50 Hz systems. The ZCD-based phase measurement achieves accurate real-time PF computation without expensive metering ICs. The two-stage capacitor switching algorithm successfully corrects PF from 0.823 to 0.994 under mixed inductive-resistive loading, reducing reactive power by 78%. The ESP32-based local web server provides platform-independent, internet-free remote monitoring accessible from any browser. With a prototype cost of approximately INR 1,500, the system is competitive with commercial solutions while offering significantly more monitoring capability. Future work will extend the design to three-phase systems, integrate true-RMS metering ICs, add MQTT cloud logging, and replace mechanical relays with TRIAC zero-voltage switches for transient-free operation

REFERENCES

1. A. E. Fitzgerald, C. Kingsley, and S. D. Umans, *Electric Machinery*, 6th ed. New York: McGraw-Hill, 2003.
2. M. H. Rashid, *Power Electronics Handbook*, 3rd ed. Burlington, MA: Butterworth-Heinemann, 2011.
3. W. H. Hayt and J. E. Kemmerly, *Engineering Circuit Analysis*, 8th ed. New York: McGraw-Hill, 2011.
4. C. K. Alexander and M. N. O. Sadiku, *Fundamentals of Electric Circuits*, 6th ed. New York: McGraw-Hill, 2016.
5. A. Patil, S. Joshi, and R. Kumbhar, "Microcontroller-based automatic power factor correction using PIC16F877A," *Int. J. Eng. Res. Technol.*, vol. 5, no. 3, pp. 421–426, 2016.
6. R. Kumar and A. K. Singh, "Arduino Mega based three-phase APFC with relay-switched capacitor banks," in *Proc. IEEE PEDES*, pp. 1–5, 2018.
7. P. Shanmugam, V. Rajesh, and K. Murugan, "Comparison of ZCD and ADC-based PF measurement for APFC systems," *IJAREEIE*, vol. 7, no. 11, pp. 3882–3889, 2018.
8. S. K. Srivastava and D. K. Palwalia, "GSM based remote energy monitoring system," in *Proc. IEEE RDCAPE*, pp. 234–238, 2015.
9. B. Rajan, S. Krishnaswamy, and T. Murugesan, "IoT-based residential energy monitoring using ESP8266 and Blynk," *IJITEE*, vol. 8, no. 6S4, pp. 1–6, 2019.
10. P. Sharma, A. Gupta, and N. Bansal, "Cloud-based APFC monitoring using ESP8266 and ThingSpeak," in *Proc. IEEE ICCA*, pp. 1–6, 2017.
11. R. Pandey and V. Agarwal, "ESP32-based real-time power quality analyzer with local web server," *IJECE*, vol. 10, no. 2, pp. 1402–1410, 2020.
12. Espressif Systems, "ESP32 Technical Reference Manual," Ver. 4.7, 2023.
13. Microchip Technology, "ATmega328P Datasheet," Rev. DS40002061B, 2020.
14. IEEE Std 519-2014, "Recommended Practice for Harmonic Control in Electric Power Systems," IEEE, 2014.
15. Bureau of Energy Efficiency (BEE), "Power Factor Improvement: A Technical Guide for Industries," Ministry of Power, Govt. of India, 2021.



INTERNATIONAL
STANDARD
SERIAL
NUMBER
INDIA



INTERNATIONAL JOURNAL OF INNOVATIVE RESEARCH

IN SCIENCE | ENGINEERING | TECHNOLOGY

 9940 572 462  6381 907 438  ijirset@gmail.com



www.ijirset.com

Scan to save the contact details